ーゲティングにも適用される。これらのキャリアの中で高分子ミセルは，このEPR効果を利用した疎水性の強い抗がん剤ターゲティングキャリアとして大変優れていると考えられる。なぜなら，EPR効果を示すためにはその大きさが5～200 nmであることが求められるとともに，その表面は親水的で荷電においては中性か弱く負に帯電していることが必要である[8]。高分子ミセルの大きさはまさしくEPR効果に適した範囲内であり，疎水性や正荷電の薬物を多量に封入しても疎水性内核を親水性の外殻がとり囲んでいるので，表面物性は親水的であり，EPR効果発現のための条件を満たしているからである。

また，この小さな粒径であることは，容易にフィルターろ過による滅菌操作を可能とし，製剤上の大きな利点となっている。

3.2.2　機能的な材料設計が容易

図1に示したように，ブロックコポリマーのA鎖がミセル外殻を形成し，B鎖が内核を形成する。ミセル外殻はタンパク質や細胞などの生体成分と相互作用を通して体内動態・分布を決定する。一方，内核は薬物を封入し，標的に到着した後の薬効発現を担う。すなわち，ブロックコポリマーのそれぞれの鎖に合目的な機能を与え，それを最適化するように化学構造を選択することができる。このように，機能分離性はシステム設計の観点から見ると大きな利点となり，内核を構成する高分子鎖と外殻を構成する高分子鎖とに薬物キャリアシステムとして必要とされる機能を分割して付与することで，より高性能のシステムが達成可能となる。

3.2.3　低い毒性

まず，高分子ミセルの生体内毒性について詳細に解明されたわけではなく，4つの臨床試験[9~11]が行われている現時点（2008年）までで，把握されている副作用がないという現状であるということをまずお断りしておく。その上で，概念的な高分子ミセルの毒性の低さから説明させていただく。

固形がんなどを標的とするターゲティングでは，血液の循環性を高めることが有益な場合が多いか，そのためには腎臓のろ過作用によって排出されない充分な大きさである必要がある。この要件を満たしたキャリアシステムは一方において，生体外へ排出されないことによる長期に蓄積毒性の懸念がある。もちろん，腎臓から排出されなくても肝臓から胆汁排泄を通しての経路もあるのであるが，腎臓からの排泄が確保されていることは，現時点では重要なことと考えられている。通常の材料では，高い血液循環性と長期的な腎臓からの排出性を両立するには，材料を生体内分解性のもので作製する必要がある。一方，高分子ミセルは，高分子の会合によってミセル構造が構築されているので，血液循環性が必要な時間範囲ではミセル構造によって腎臓からの排出を免れ，長期的に見れば高分子ミセルは1本1本の高分子鎖に解離するため，生体に蓄積して毒性を及ぼす心配が概念上ないことになる。そのための設計としては，ミセルから解離したブロッ

クコポリマーの分子量を腎臓から排出されるように（約3万以下にする）することである。

次に，筆者が研究・開発に関係したシステムについての毒性について述べる。まず，マウスがんモデルを用いた評価では，最大耐量を基準に評価を行うため，非選択的に正常組織・臓器に分布した抗がん剤による副作用が顕著に起きている状態での評価であり，高分子ミセルキャリア自体の毒性を評価することは困難な場合が多い。また，実験動物で知ることのできる副作用はかなり限られている。このような限られた範囲の評価であっても，内包する抗がん剤が元々有していた副作用と異なるタイプの副作用が見られるかは大切な事項である。これまでの検討ではそのような副作用は観察されることはなかった[12~16]。

薬物ターゲティングの臨床では，キャリア自体，あるいはキャリアによるターゲティングの特性によって元来の抗がん剤にはない特有の副作用が報告されている。リポソーム製剤におけるhand and foot syndromeであり，抗体製剤におけるinfusion-related reactionがよく知られた例である。これまでに明らかになった高分子ミセル抗がん剤の臨床報告では，キャリアシステム特有の副作用は観察されていない。

以上の結果を持って，「高分子ミセルキャリアには毒性はない」とか「抗がん剤を対象とした場合には全く問題はない」とするには，更なる基礎的・臨床的な検討の積み上げが必要である。しかし，少なからず行われた動物実験・臨床試験の中で毒性が認められないという事実は，毒性面から見た高分子ミセルの高いポテンシャルを示していると考えられる。

3.2.4　様々なタイプの薬物封入が可能

これまでは，疎水性のミセル内核に疎水性の低分子薬物を封入するタイプを中心に説明を行ってきた。薬物には疎水性部分を含むものが多いので，疎水性相互作用を利用することが最も適用範囲が広いためである。しかし，高分子ミセルを形成する性質（ミセル内核の会合を生み出す相互作用）は疎水性相互作用に限定されない。一般的には疎水性内核には限定されず，水系の溶媒中，内核でB鎖が会合を起こすような相互作用を起こせばミセル形成し得るということである。この相互作用としては上述の疎水性相互作用の他には，静電相互作用，水素結合などがある。静電相互作用，水素結合を利用すれば，DNAやタンパク質などの高分子をミセルに封入することに応用できる[17,18]。また，金属錯体の抗がん剤であるシスプラチンを結合させた高分子ミセルシステム[19,20]がある。結合させたシスプラチン自身，ある程度の疎水性を有するが，ミセル形成の中心的な役割を果たしているのが高分子鎖間の架橋構造であることが他の場合と異なっている。シスプラチン分子中心の白金イオンに複数の高分子側鎖が配位結合して，高分子間に架橋構造が生ずることでミセル内核が形成している。

次に高分子ミセルキャリアの短所と考えられる２つの事項を述べる。

3.2.5　比較的高度な高分子合成が必要

典型的な高分子ミセルを得るためには，合成高分子としては珍しい部類のブロックコポリマーが必要であり，ブロックコポリマーを合成する方法はそうでないポリマーを合成する方法よりも高い技術が必要とされる場合が多い。高分子合成はその単位であるモノマーと呼ばれる低分子化合物を連鎖的に結合して行く反応で得る。よって，図３に示すようにAのモノマーの重合（連鎖的結合反応）が終了した頃を見計らって，別の種類のモノマーBを加えれば容易にAB型のブロックコポリマーが得られると想像するのは自然なことである。しかし現実には，様々な副反応が起こり，目的とするAB型のブロックコポリマーはほとんど得られず，図３の下側に示したAやBのみから成るホモポリマーや，分岐した形のポリマーが生成してしまう。大部分の合成高分子の生産に用いられているラジカル重合法では，非常に特殊な触媒系を用いない限り，このような副反応は避け得ず，通常ブロックコポリマーを得る方法としては機能しない。アニオン重合法といった副反応が少ない方法でのみ，ブロックコポリマーは合成できる。また，どのモノマーもアニオン重合などブロックコポリマー合成に適する方法で重合するとは言えず，用いることのできるモノマー種類はある程度限定を受ける。

また，単に高分子ミセルを形成すれば必ず薬物キャリアとして有用というわけではなく，ブロックコポリマー化学構造にかなり左右されることも，高分子合成化学が重要であることを示している[21]。逆に見ると，高分子合成化学の技術がない環境での高分子ミセルキャリア研究・開発が遂行しにくいことであり，大きな進歩を得るためには短所であると考えられる。

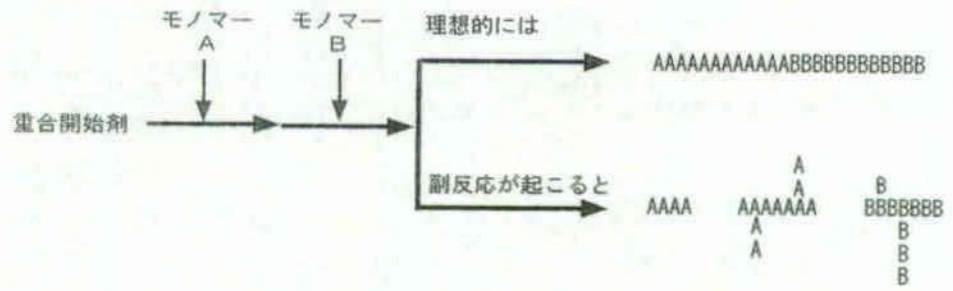

図３　ブロックコポリマーの合成

3.2.6　薬物封入法が未発達

マイクロスフィアやリポソームなど研究と開発の歴史が長いキャリアシステムに比べて，新しい高分子ミセルでは，薬物を安定にかつ高効率でミセル内核に封入する方法[3,22~24]についての

検討が未発達である。また，実験室でのスケールではうまく封入できても，それを臨床に向けたスケールに大きくする方法論も今後進歩させる必要を感じる。

3.3　高分子合成

高分子ミセルキャリアの設計・作製のための，高分子化学をここで詳述することはスペースの関係で不可能である。高分子化学の教科書を参照していただくより他ない。ただし，ここでは高分子ミセルキャリアのために最も基礎的かつ重要である２点を説明させていただく。

3.3.1　ブロックコポリマーを合成する意味

3.1項の「高分子ミセル薬物キャリアとは」にも解説したように，高分子ミセルを形成する高分子の形態はブロックコポリマーに限定されないが，現在までのすべての臨床開発，大部分の基礎研究はAB型あるいはABA型のブロックコポリマーを用いてなされている。前項3.2.5に記述したように，どのような高分子鎖の組み合わせでも自由にブロックコポリマーが合成できるわけではなく，合成できる鎖の種類の組み合わせとそれを得る方法（重合法）は限定される。また，ブロックコポリマー合成においてA鎖やB鎖のホモポリマーが不純物として混入する場合がある。水溶性のA鎖はミセル形成挙動に影響は少ないが，ミセル形成部分であるB鎖のホモポリマーはミセル形成挙動への影響が大きいので，なるべく除きたい不純物である。

3.3.2　分子量のそろったポリマーを合成すること

天然高分子であるタンパク質は，ある種類のものには１つの分子量しか存在しない。これに対して合成高分子の分子量には分布があり，その平均分子量と分布の広がり度合いで表現される。高分子ミセルとしての粒径などの物性を正確に得るためにも，また医薬品としての品質管理のためにも，この分子量分布は狭いものが求められる。この分子量分布の狭さ　広さは，重合の種類とモノマーの種類によって大きく左右される。よって高分子ミセルキャリアのためにはこの面でも好適な（分子量分布の狭い）高分子鎖が選択される。大部分の研究・開発システムのミセル外殻高分子として用いられているポリエチレングリコール（PEG）鎖は，分子量分布の最も狭い代表的な合成高分子である。また，筆者らがミセル内核構成高分子鎖として用いているポリアミノ酸も，PEGに次いで狭い分子量分布が得られる。

以上述べたように，高分子ミセルキャリアのために使用できる高分子鎖の種類は高分子合成の観点からの制限を受ける。ただし，最新の合成技術を用いれば，それ程数多くの研究開発がなされていない現時点では，充分な種類の高分子鎖が選択され得る（つまり検討されていない高分子鎖の組み合わせは充分に多い）と言える。

3.4　高分子ミセルにおける製剤設計の諸要素

3.4.1　高分子鎖の長さ

AB型のブロックコポリマーから高分子ミセルを形成させるとき，そのミセル構造形成挙動を決める大きな要因は，高分子鎖の長さである。ここではA鎖を親水性のブロック，B鎖を疎水性ブロックとして話を進めさせていただく。親水性A鎖が長く，疎水性B鎖が短い場合には，ブロックコポリマーが単独で水中に可溶化して，ミセル構造は形成しない。それよりもA鎖が短く(相対的あるいは絶対的長さにおいて)，B鎖が長くなるとミセル構造を形成するようになる。さらに，A鎖が短くB鎖が長くなると水に不溶の凝集となってしまう（ミセル構造よりもA鎖が短くB鎖が長い側に，ポリマーソーム構造[注2]を形成する場合がある)。よって，ある範囲内にA鎖長とB鎖長があるときに，高分子ミセルが形成することになる。この鎖長の範囲は両高分子鎖の化学構造によって規定される。例えば，より疎水性の強いB鎖を用いた場合には，よりB鎖が短い範囲でミセルが形成される。

以上は，ミセル形成の物理化学では基本的なことであるが，薬物キャリアとしてはそのミセル形成範囲内では，高分子としてどのような構造のものを用いるのが好ましいのであろうか？　結論から申し上げるとこの点の解明は行われていないのが現状である。しかし，いくつかわかっていることがある。

高分子鎖の長さを変えたときに変化する高分子ミセルの基本的物性は，臨界ミセル濃度(CMC)と粒径である。ミセル構造を形成する高分子鎖の範囲内で，疎水性の高分子鎖を長くすると，CMCは小さくなる。また，粒径は一般的には大きくなる。この粒径増大は，疎水性部分が大きくなったことにより，主に1個のミセルを構成する会合ポリマー数が増大するためである。前項3.1で説明した通り，血液中のデリバリーにおけるCMCの重要性が解明されていないため，ブロックコポリマー組成を変えたときに，CMCと粒径の両方が変化して，薬物動態への影響が解析できないことが大きな理由である。しかしながら，いくつかの有益な情報は得られている。

著者らが行った抗がん剤アドリアマイシンを内包させた高分子ミセル[15]では，親水性（外殻になる）のポリエチレングリコール鎖が長く，疎水核になるポリアミノ酸誘導体の短いものが高い抗がん活性を示した。この例では，疎水性鎖はポリアスパラギン酸に疎水性の抗がん剤アドリアマイシンを化学結合することによって得ている。よって，アスパラギン酸残基のどのくらいの割合にアドリアマイシンを結合させるかで，ポリアミノ酸誘導体鎖の疎水性の強さは変わってくる。このアドリアマイシンの高分子ミセルでは，かなりの長さの範囲でミセル構造を形成させるために，結合率を変えて高分子を得ている。このように高分子鎖長の正確な比較にはなっていな

注2）ポリマーソームとは，脂質から成るリポソームのように高分子でベシクル構造となるもの。

いのであるが，興味あるのは最も高い*in vivo*抗がん活性を示したのは最も親水性PEG鎖が長く，疎水性鎖が最も短いものであった。そのうちの代表的な組成の体内動態を比べてみると，最も抗がん活性の高かった組成が最も長い血中半減期と，高いがん集積性を示していた。このことは，血中循環性の高い組成のミセルが，最も効率よくEPR効果に基づいたがんターゲティングを実現できるので，高い抗がん活性を示すことが可能となることを示す。高分子ミセル形成高分子の鎖長がどのような要因で，高い血中循環性を示すようになるかについての考察は3.4.4において行う。

3.4.2　ミセル内核形成高分子鎖の化学構造

疎水性の薬物を封入するためと，水溶液でミセル形成するために，ミセル形成高分子B鎖は疎水性であることはもちろんであるが，単に疎水性がミセル形成と薬物封入に足るのに充分であれば，ターゲティングが達成できるわけではないことがはっきりしている。

抗がん活性物質カンプトテシン封入高分子ミセル[21, 25, 26]では，ミセルを形成する高分子鎖が中間的な疎水性のときに特異的に高い血中循環性を示した。カンプトテシンはほとんど水に溶解しない疎水性の化合物であるので，疎水性相互作用が主たる薬物封入の相互作用であることは自明であり，ある程度範囲の疎水性を有する高分子鎖のミセルへの封入は比較的容易であった。にもかかわらず，特定の疎水性度のもののみ高い血中循環性を示した事実は，血液中の高い血中循環性を得るためには，それ以外の因子が封入には必要であることを意味する。その因子として第一に考えられるのは，高分子鎖に薬物がよくからみつくような立体的なスペースが高分子構造にあることである。しかし，結晶でもないこのような立体的な因子を解析することは困難である。

アドリアマイシンを封入して固形がんへのターゲティングに成功した組成[15, 16]においても，上記で述べた立体的な要因が好適に達成された組成である可能性がある。アドリアマイシンの場合はそれに加えて，アドリアマイシン分子間で相互作用して非共有結合的な2量体構造が作りやすいことが知られている。この薬物封入は高分子鎖に化学結合したアドリアマイシン分子に，他のアドリアマイシン分子が物理的に吸着することによっている。単に水分子と接することを嫌う分子同士が集まる疎水性相互作用のみではなく，分子同士が特異的とも言える親和性を有していることが，アドリアマイシンのシステムでは有効に作用している可能性がある。

ある化学構造の疎水性薬物を高分子ミセルに封入してターゲティングしようとしたとき，薬物封入が可能な高分子組成を見つけることは容易であるが，高い血中循環性を示すように安定に薬物を封入できる高分子組成を見つけることは容易でない。高分子ミセル薬物キャリア研究の最重要部分は封入安定性を高める高分子組成を見つけることにあると言っても過言ではない。このように，任意の薬物封入を最適化できる高分子を容易に見つけるための方法論を構築することが大切である。そのためには，基礎的な高分子化学，物理化学，分析化学にまで範囲を広げた研究が

必要であると考えられる。

3.4.3　封入薬物量

ミセルを形成する高分子鎖が固定された場合，それに封入する薬物量はターゲティング性能に影響するのであろうか？　これについては影響する場合と，影響しない場合が知られている。

まず，封入薬物量がターゲティングに影響するアドリアマイシン封入ミセルの例[16]を紹介する。この例では，ブロックコポリマーを固定して，物理的に封入するアドリアマイシンの量を変えて，抗がん活性および体内動態を比較している。この物理的封入薬物量が多い方が，血中循環性が高く，より固形がんに集積し，抗がん活性もより高い。この事実は，封入薬物がミセル内核の環境をより疎水的にすることで，薬物の封入安定性が向上したと考えられる。このアドリアマイシンの場合には，intactなアドリアマイシンよりも疎水性の高いアドリアマイシン２量体が形成してミセルに封入されているという，特殊な事実があるが，この２量体がミセル内核の疎水性を高めることは事実である。

一方，カンプトテシン封入ミセルではその封入量をブロックコポリマーに対して５～40%の重量割合にした範囲では，薬物の血液循環性には変化が見られない[25]。薬物封入の安定性は疎水性高分子鎖と薬物間の相互作用によって決まり，薬物封入に伴う内核の環境変化は影響しない状態のように考えられる。

以上のように，封入薬物量に関しては対照的な場合があることが知られているが，どのような化学的要因によって，どちらになるかについては不明である。しかし，少なくとも薬物封入量はターゲティングを決定する重要な要因になる可能性があり，検討すべき因子であることは確かである。

3.4.4　ターゲティング性能と高分子ミセルの物理化学物性との関係

上記の3.4.1～3.4.3では高分子ミセルキャリアシステムの化学組成を決める要因について述べてきた。これらの化学組成は図４に示すように，体内でのミセル粒径，構造安定性，表面物性，薬物放出速度によって体内動態・分布が決定されていると考えられる。このうち構造安定性は様々な要素を含む。3.1の「高分子ミセル薬物キャリアとは」の項で述べたように，動的および静的なミセル構造安定性が影響し得る。また，生体では構造的に安定でも，肝臓や脾臓などの細網内皮系に捕捉されることで血液中濃度が急速に低下して，望むターゲティングは達成できない。

図４の化学構造，ミセル物性，ターゲティング性能の関連を解析し，よりよきターゲティング性能を得る道筋を見つけることが，高分子ミセルによるターゲティング研究・開発の核心部分と言える。これらの道筋はよくわかってないことが多い状況であるが，その中で，明らかになった道筋が１つある。それは，水系ゲルパーミエーションクロマトグラフィー（GPC）での封入薬物

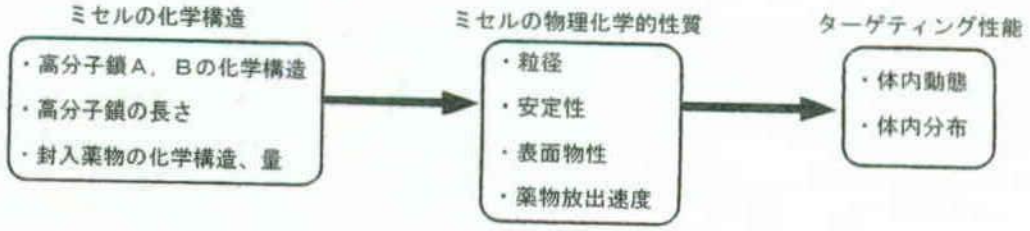

図４　高分子ミセル薬物キャリアシステムの設計

の測定である。水系のGPCでは疎水性の薬物は，水に溶解しないために測定ができないか，もし多少の水溶性を示すことでカラムに注入できても，カラムとの疎水性相互作用のために吸着して検出されないか，非常に遅れて流出する。一方，高分子ミセルはその分子量が数百万に対応する大きさであり，通常カラムの排除体積に（つまり一番早い流出時間で）流出する。また，高分子ミセルが真のカラムの排除体積に流出するのは，カラムとの疎水性相互作用が全くない場合である。以上の事柄を総合すると，封入薬物が早い流出時間で大きなピークで流出するほど，ミセルへの封入は安定であり，ミセルも疎水性相互作用を及ぼすことが少ないと言える。

これまでに，水系のGPCで評価した*in vitro*のミセルとしての優劣（薬物封入高分子ミセルのピークが早くて大きい程よいとする）が，*in vivo*での血液中循環性，がん集積性，および抗がん活性の優劣と一致する例[27,28]が複数知られている。逆に，この関係から外れた例は経験した高分子ミセルシステムではなかった。このことは，高分子ミセルによるパッシブターゲティングにおいては，内包する薬物に起因する疎水性相互作用をいかに完璧にミセル内核に封じ込めて，タンパク質や貪食性細胞との相互作用を抑制することが第一に重要であるかということを示唆する。

3.5　おわりに

本節では，高分子ミセル薬物キャリアの製剤設計各要素についてまとめた。本キャリアシステムは，製剤設計において水溶性高分子，リポソームなどの他のキャリアシステムとは大きく異なる面があることを述べた。また，比較的に高度な高分子合成が必要なことなど，急速な発展を阻害する要因についても述べた。それにもかかわらず，ターゲティングで果たし得る大きな可能性を考慮すれば，技術的な困難を克服して研究・開発する価値のあるキャリアシステムであると信じる。

文　献

1) M.Yokoyama, "Nanoparticles for Pharmaceutical Applications", p.63, American Scientific Publishers (2007)
2) M.Yokoyama, "Drug and Pharmaceutical Sciences, vol.148, Polymeric Drug Delivery Systems", p.553, Taylor & Francis (2005)
3) H. M. Aliabadi and A. Lavasanifar, *Expert Opinion on Drug Delivery*, 3, 139 (2006)
4) Y. Geng *et al.*, *Nature Nanotechnology*, 2, 249 (2007)
5) M. Wilhelm *et al.*, *Macromolecules*, 24, 1033 (1991)
6) Y. Matsumura and H. Maeda, *Cancer Res.*, 46, 6387 (1986)
7) H. Maeda *et al.*, *Bioconjugate Chem.*, 3, 351 (1992)
8) 横山昌幸，ナノ粒子とドラッグターゲティング，機能材料，22，22-27 (2002)
9) Y. Matsumura *et al.*, *Br. J. Cancer*, 91, 1775 (2004)
10) T. Hamaguchi *et al.*, *Br. J. Cancer*, 97, 170 (2007)
11) 濱口哲弥，血液・腫瘍科，54，702 (2007)
12) T. Hamaguchi *et al.*, *British J. Cancer*, 92, 1240 (2005)
13) M. Yokoyama *et al.*, *Cancer Res.*, 50, 1693 (1990)
14) M. Yokoyama *et al.*, *Cancer Res.*, 51, 3229 (1991)
15) M. Yokoyama *et al.*, *Drug Delivery*, 1, 11 (1993)
16) M. Yokoyama *et al.*, *J. Drug Targeting*, 7, 171 (1999)
17) K. Kataoka *et al.*, *Macromolecules*, 29, 8556 (1996)
18) A. Harada *et al.*, *Macromolecules*, 31, 288 (1998)
19) M. Yokoyama *et al.*, *J. Controlled Release*, 39, 351 (1996)
20) H. Uchino *et al.*, *Br. J. Cancer*, 93, 678 (2005)
21) T. Yamamoto *et al.*, *J. Controlled Release*, 123, 11-18 (2007)
22) G. S. Kwon *et al.*, *Colloids and Surfaces, B: Biointerfaces*, 2, 429 (1994)
23) M. Yokoyama *et al.*, *J. Controlled Release*, 32, 269 (1994)
24) M. Yokoyama *et al.*, *J. Drug Targeting*, 12, 373 (2004)
25) M. Watanabe *et al.*, *International J. of Pharmaceutics*, 308, 183 (2006)
26) K. Kawano *et al.*, *J. Controlled Release*, 112, 329 (2006)
27) M. Yokoyama *et al.*, *J. Controlled Release*, 28, 59 (1994)
28) M. Yokoyama *et al.*, *J. Controlled Release*, 50, 79 (1998)

機能性DDSキャリアの製剤設計

2008年10月10日　第1刷発行

監　修　岡田弘晃　(T0642)
発行者　辻　賢司
発行所　株式会社シーエムシー出版
東京都千代田区内神田1-13-1（鹿島屋ビル）
電話 03 (3293) 2061
大阪市中央区南新町1-2-4（椿本ビル）
電話 06 (4794) 8234
http://www.cmcbooks.co.jp/

〔印刷　株式会社遊文舎〕

定価はカバーに表示してあります。
落丁・乱丁本はお取替えいたします。

ISBN978-4-7813-0052-8 C3047 ¥65000E

In: Cancer Metastases Research
Editor: Akira Watanabe, pp. 147-163

ISBN: 978-1-60456-130-2

Chapter VI

Demonstration and Partial Identification of Aberrant Muc1 Bearing Tn Antigen in Rat Ascites Hepatoma AH109A Cells with Strong Lymph Node Metastasis Propensity

***Takanori Kawaguchi*[*1, 5], *Shunsuke Imai*[2], *Satomi Haga*[3], *Jyunji Morimoto*[4] *and Takashi Honda*[5]**

[1]Department of Pathology, Aizu Central Hospital, Aizu Wakamatsu 965-8611
[2]Division of Pathology, Nara City Hospital, Nara 630-8305, Japan
[3]Nara Prefectural Institute of Public Health, Nara 630-8131, Japan
[4]Experimental Animal Center, Osaka Medical College, Osaka 569-8686, Japan
[5]Division of Human Life Sciences, Fukushima Medical University School of Nursing, Fukushima 960-1295, Japan

Abstract

Lymphatic metastasis is a crucial property of malignant tumors, but little is known about the molecular mechanism associated with this feature. We recently discovered an aberrant MUC1 of ~33 kDa bearing *Vicia villosa agglutinin* (VVA)-binding carbohydrate(s) (Tn antigen). Expression of the MUC1 protein in cancer cells had a significant relation to lymph node metastasis in patients with breast cancer (Current Drug Targets, 2005; Breast Cancer Res Treat, 2006). At present, we are investigating aberrant MUC1 bearing Tn antigen of rat ascites hepatoma AH109A cells (poorly differentiated hepatocellular carcinoma) with strong lymphatic metastasis propensity. These cells metastasized to lymph nodes 2 to 3 weeks after the inoculation into subcutaneous tissue of abdominal wall when intercellular adhesion molecule 1 (ICAM-1) appeared in

* Address correspondence to Dr. Takanori Kawaguchi at the Division of Human Life Sciences, Fukushima Medical University School of Nursing, 1 Hikariga-oka, Fukushima 960-1295, Japan; Tel: +81-24-548-7151; e-mail: t-kawa@fmu.ac.jp

malignancy of various kinds of cancers [9-13]. Alternation of MUC1 localization in the cells is severely related to metastatic propensity of cancer cells [14, 15]. We have demonstrated that lack of heterozygosity of MUC1 protein of primary breast cancer cells is related to lymph node metastasis status of the patients [16]. More recent our studies demonstrated a relationship between expression of low molecular aberrant MUC1 proteins of primary breast cancer cells and lymph node metastasis status of the patients [17, 18]. Among MUC1s with varying molecular weights, ~33 kDa MUC1protein was considered to be most relevant to lymphatic metastasis. We were also interested in unique carbohydrate(s) bore with the ~33 kDa MUC1, which binds to *Vicia villosa* agglutinin (lectin) (VVA). VVA is known to be a lectin, which binds specific to *N*-acetylgalactosamine, especially strong to Tn antigen [19, 20].

Through considerations of literatures and our own researches, we think that animal tumor model is necessary to elucidate the role of MUC1 of cancer cells on metastasis. Regretfully, little information on MUC1 has been provided in experimental animal tumors, although some xenograft models contribute to understanding of metastasis [21, 22]. In the present paper we investigate MUC1 of rat ascites hepatoma AH109A cells, which metastasize preferentially to lymph nodes.

Materials and Methods

Animal and Tumor

Four- to six-week old rats (60 to 80 g) were purchased from Chares River (Tokyo, Japan). Rats were maintained under water *ad libitum* and were used for the experiments. Experiments were carried out under the control of the Animal Research Committee in accordance with the Guidelines on Animal Experiments in Fukushima Medical College and Japanese Government Animal Protection and Management Low.

Rat ascites hepatoma AH109A was used. This is an ascites form cell line of poorly differentiated hepatocellular carcinoma, syngeneic to Donryu strain rat, and has been cryopreserved in our laboratory [23]. The cell line usually was maintained by intraperitoneal (ip) transplantation during experiments. On the 7 day after inoculation, ascites was obtained and washed several times with physiological saline solution (PB) to remove erythrocytes. It was confirmed by trypan blue exclusion test that more over 90% of tumor cells were alive. A tumor cell suspension (2.0×10^6 cells in 0.2 ml of PB) was used to experiments. All animals used were autopsied at the time of death or at 3 months after the inoculation.

Histology and Immunohistochemistry

Histological materials were fixed ordinary in 10% formalin containing 4% methanol. Fixations using 4% paraformaldehyde or zinc (Zinc Fixative, formalin-free; BD Pharminogen, San Diego, CA, USA) under the condition of whole body circulation were also carried out in some cases. Materials were embedded in paraffin and sections with 3 μm thickness were made. These thin sections were placed onto glass slides, deparaffined in

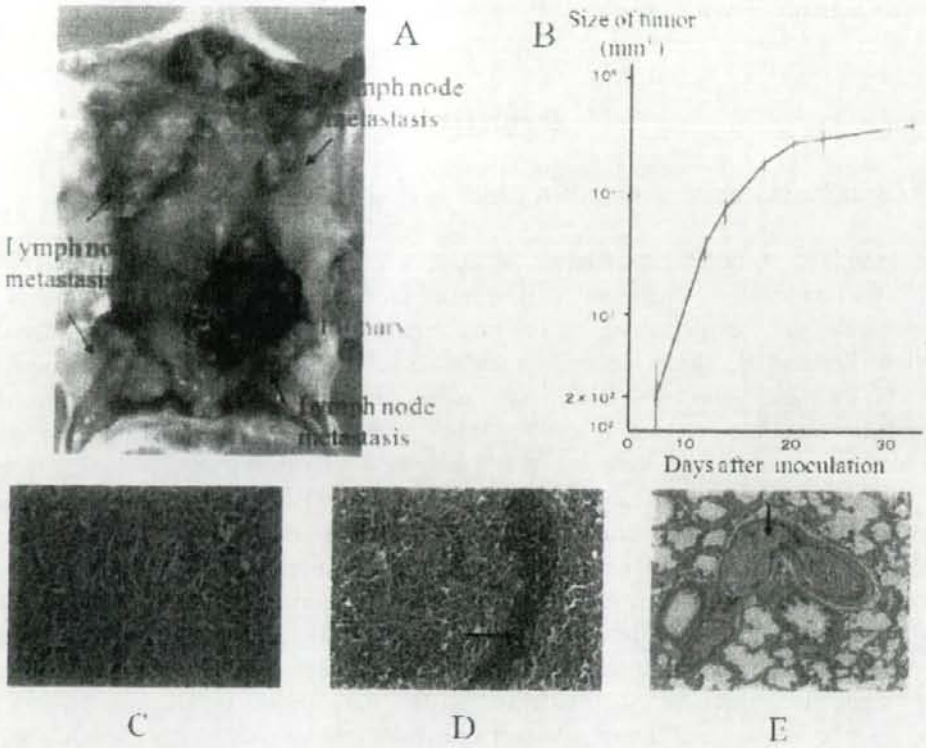

Figure 1. Morphological appearance and growth curve of AH109A tumors. A: Primary lesion in sc tissue of abdominal wall and its metastasis in lymph nodes of axillary, inguinal and neck regions. B: Growth curve of AH109A tumor inoculated sc. An average value with standard deviation of 8 animals was indicated). C, D, and E: Histological appearances of AH109A cells in primary sc tumor, lymph node, and lung, respectively. Arrow heads of D and E indicate lymphocytic infiltration around tumor cells and tumor cells in pulmonary artery, respectively. Original magnifications for C, D and E are ×400, ×200 and ×200, respectively.

The homogenized suspensions were centrifuged at 3,000 rpm for 10 min to remove the crude sediments and supernatants were shaken gently at 4°C overnight. The solutions were dialyzed against 10 mM PB at 4°C overnight and protein fractions were salting- out by ammonium sulfate (Wako, Osaka, Japan). The sediment protein was harvested by centrifugation (10,000 rpm, 15 min), and were concentrated using a molecular size cut-off membrane filter of 10 kDa (Ultracent-10 Tosoh, Tokyo, Japan or VIVASAPINAE 20, VIVASCIENCE, Hannover, Germany), to a concentration of 5mg/1ml PB. The protein concentration was measured by using a BCA Proteins Assay kit (Pierce, Rockford, IL). The suspension was passed through a Blue sepharose column (Seikagaku Industry Co., Tokyo Japan) to remove serum albumin. After concentrated, the specimens were stored at a -80° C deep freezer.

Submandibular glands of adult female rats were homogenized in an earthenware mortar and the homogenized materials were treated as described above.

temperature, followed by incubation at 4°C overnight with gently shaking. The solution was centrifuged at 10,000 rpm for 15 min and the supernatant was used for staining.

Results

Growth and Metastasis of AH109A Cells

We examined metastatic preference of AH109A cells by injecting the cells into subcutaneous (sc) tissue of abdominal wall of rats, and the results were shown in Figure 1. The tumor cells grew exponentially in the rats resulting in death until 65 days after the inoculation [Figure 1B]. These rats had lymph node metastases in axillary and/or inguinal regions. In addition, some rats had lymph node metastasis in the neck, paratrachea, retroperitoneum, and mesenterium [Fig. 1A]. When sc tumors were resected at 1week after the inoculation, metastasis did not occur at all (none of 4 rats) in any sites including lymph nodes, whereas lymph node metastases occurred in all animals (4 of 4 rats) examined when tumors were resected at 3 weeks after the inoculation. When primary tumors were resected at 2 weeks after sc inoculation, lymph node metastasis occurred in 2 of 4 rats examined. Microscopically, tumor cells grew in sc tissues accompanying abundant blood vessels within 1 week after the inoculation (Figure 1C), and thereafter drastic changes occurred in the stroma of tumors and peritumoral tissues, such as extensive necrosis, sinusoidal vasculatures, fibroblastic and myofibroblastic cell proliferations (data, not shown).

Intravascular migration of tumor cells were easily detected 3 weeks after the inoculation and metastatic tumors were detected in lymph nodes and the lungs of all animals died with tumors. Tumor cells were found to grow well in lymph nodes and formed solid tumors [Figure 1D], while metastatic tumors in the lung, except for 2 animals, were very small and frequently localized in pulmonary arteries [Figure 1E). Adrenal gland metastasis was found in 2 of 10 rats died with tumors, but no tumor metastasis was found in any other organs, such as brain, heart, liver, kidney, muscle, bone, and others.

Intravenous injection of the cells (2×10^6) into rat (8 rats) did not produce metastatic nodules in any organs including the lungs until 3 weeks after the injection when these rats were sacrificed at this time.

Immunohistochemical and Lectin Histochemical Expression of MUC1, Vicia Viosa Agglutinin (VVA)-Binding Carbohydrates, and Intercellular Adhesion Molecule 1(ICAM-1)

Three kinds of MUC1 antibodies (C-20, H-295, and N-19) displayed differential immunostaining of AH109A tumor cells grown in sc tissues. C-20 antibody-positive staining was found in the cytoplasm of tumor cells as diffuse fine granules [Figure 2A]. On the other hand, C-20 antibody stained large droplets in tumor cell cytoplasm, which appeared mainly in the late stage of tumor growth [Figure 2C].

The tumor cells, which contained these droplets, resembled signet-ring cell carcinoma of human origin. H295-positive substances usually appeared to be deposits in the cytoplasm of tumor cells [Figure 2B], while in some areas these substances appeared to be membranous on tumor cell surfaces. We examined H-295-immunostaining on normal liver and salivary gland. It was clearly demonstrated that this antibody did not react with hepatocytes at all, while the antibody reacted strong with apical site of intrahepatic bile duct [Figure 2D]. Positive H-295 sign for salivary glands was found mainly secretory products in the lumen [Figure 2E]. Positive ICAM1-staining was found selectively in vascular endothelial cells, which appeared in 2-week-old sc tumors, but the positive sign was not found in vascular endothelial cells around 1-week-old sc tumor [Figure 3]. VVA from E.Y. Laboratories and VVA-B_4 from Sigma stained intensely the cytoplasm of tumor cells [Figure 4].

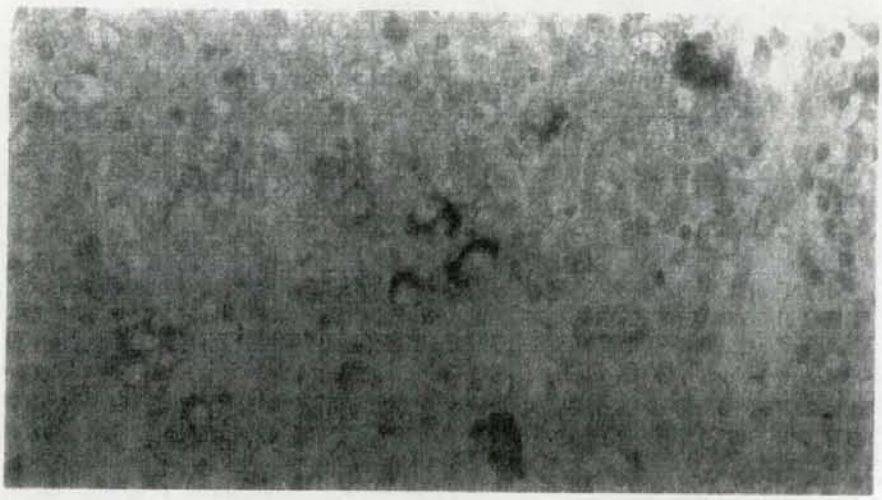

Figure 4. Expression of Vicia villosa agglutinin (VVA)-binding carbohydrate(s). VVA labeled with digoxigenin (DIG) was detected by mouse anti-DIG monoclonal antibody (Roche). ×400.

Western Blotting Profiles of Proteins Obtained from VVA Affinity Chromatography and PNA Affinity Chromatography

Since Western blot analysis on sc tumors and metastatic tumors in lymph nodes did not demonstrate clearly H-295 anti-MUC1- positive bands, we analyzed materials from VVA affinity chromatography and PNA affinity chromatography.

The elution pattern of AH109A cell lysates from sc tumors via VVA affinity chromatography was shown in Figure 5A. The sample prepared with non-reducing and denaturing condition made major H-295 reactive bands of ~40 kDa, followed by ~20 kDa and ~221 kDa [Figure 5B]. On the other hand, the sample prepared with reducing and denaturing condition made H295-reactive bands of ~ 20, ~30, ~33, and 35 kDa [Figure 5C]. The proteins from VVA affinity chromatography were too little to study the profile of these proteins. Since it is well known that PNA binds to MUC1 [See Ref 16, 18], we carried out

This showed clearly that much amounts of proteins were eluted by this procedure. So, we carried out further studies on the MUC1 obtained by PNA affinity chromatography. The results were shown in Figure 7B, demonstrating that major H295-positive molecules were located at ~30, 33~35 and ~40 kDa on sc primary tumor, and ~30, ~33~35, 40, and 50~70 kDa on metastatic tumors from lymph nodes.

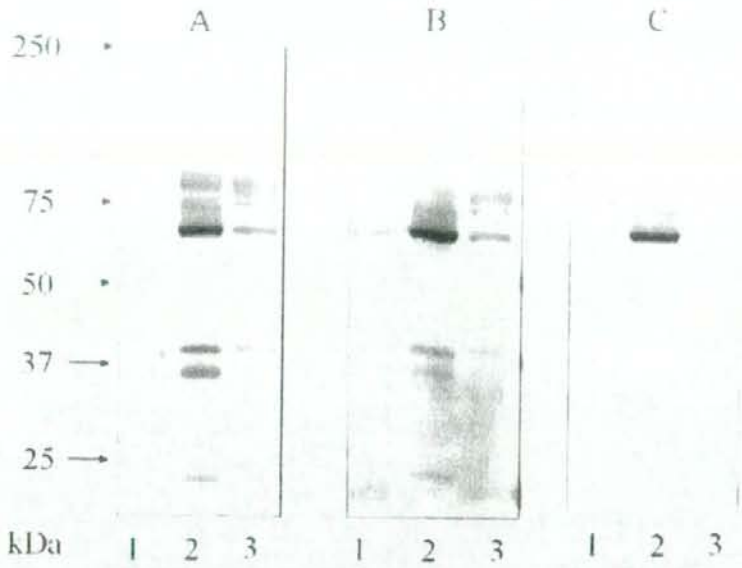

Figure 7. Hapten inhibition of Vicia villosa agglutinin-binding protein of AH109A cells by N-acetylgalactosamine and Tn antigen. A, B, and C indicate the solutions which were preincubated with 10 mM PBS, 100 mM N-acetylgalactosamine (GalNAc), or 1 mM Tn antigen (GalNAc-O-Ser/Thr), respectively. Lane1, 2 and 3 indicate submandibular gland mucin, lymph node metastasis, and primary sc tumor, respectively.

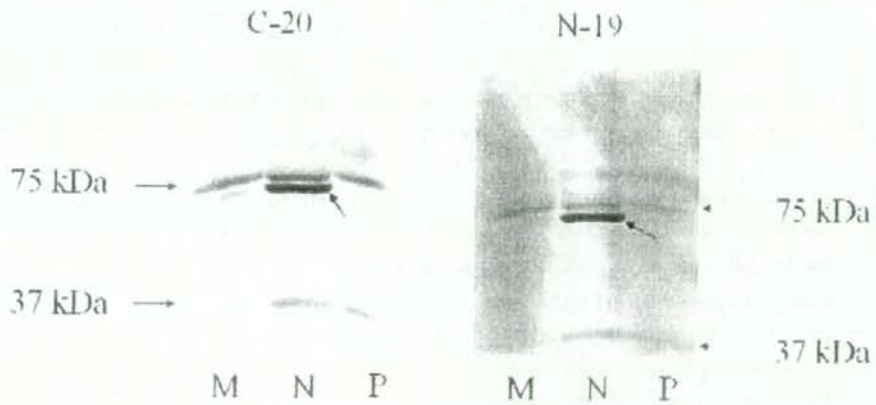

Figure 8. Western blotting profiles of C-19 and N-20-reactive proteins of AH109A cells. M, N, and P indicate submaxillary gland mucin, metastatic tumor in lymph node, and primary tumor, respectively. About 70 kDa bands indicated by an arrow head are intrinsic alkaline phosphatase derived from lymph nodes.

contains SEA module [4. 29, 30]. It is reported that the primary cleavage site of MUC1 is SEA module as FRPG/SVVV a sequence that is highly conserved in a number of heavily glycosylated mucin-like proteins [30]. It is possible to consider, therefore, that aberrant MUC1 proteins of 30~40 kDa from rat ascites hepatoma AH109A cells involve SEA module, although precise amino acid sequences of the MUC1 proteins must await further studies. This possibility suggests that aberrant MUC1 proteins of 30~40 kDa are produced not only by splicing but also by proteolysis of MUC1 proteins at SEA module.

Another important problem is of glycosylation of MUC1 proteins of 30~40 kDa. It is well known that MUC1 bears mainly O-glycosylated carbohydrates [4]. This is because VNTR domain is heavily O-glycosylated. Aberrant MUC1 proteins of 30~40 kDa bear VVA-reactive carbohydrate(s) and we have considered the carbohydrate(s) being O-glycosylated, because the VVA-reactivity was absorbed clearly by pre-incubation with Tn antigen (GalNAc-O-Ser/Thr) as seen in the previous paper [18] and in the present paper. However, there remains a possibility that the aberrant MUC1 proteins bear N-type carbohydrate(s), because VVA have strong adhesion affinity to proteins with N-type carbohydrates such as transferrin [26]. If the aberrant MUC1 proteins of 30~40 kDa involved VNTR and extracellular sequence of C-terminal subunit, it may be possible that these proteins have either O-glycosylated or N-glycosylated carbohydrates.

In any way, it is certain that MUC1 protein of rat ascites hepatoma is deviated from normal one in terms of distribution in the cells and protein composition. This can be seen in MUC1 proteins which react with C-20- and N-19-antibodies. Distribution of C-20-positive fine granular deposits in the cells [Figure 2A] is familiar in many papers that were recently reported, and N-19-reactive droplets in the cells (Fig. 2C) are reasonable feature of MUC1 accumulation in cells, although the feature was rarely reported. However, striking feature was given by Western blotting as shown in Figure 8 in which electrophoresis patterns by C-20-antibody and N-19 antibody were extremely resembled. At present, we do not know the reason.

As demonstrated by several previous workers, there is a distinct relationship between atypical expression of MUC1 of carcinoma cells and poor outcome of patients with hepatocellular carcinoma [13, 31]. Regretfully, no one knows how MUC1 of hepatocellular carcinoma cells is concerned with their malignant nature. We do not study this problem in detail, but we think that MUC1 of AH109A cells is involved in their lymph node metastasis formation in following two events in a metastatic process; intravasation and growth. The former is derived from the fact that AH109A sc tumor metastasized to lymph nodes 2 weeks after the inoculation when ICAM- 1 was expressed in vascular endothelial cells around the tumors. Since it is well- known fact that MUC1 molecule is able to bind to ICAM-1 [32, 33], the interaction may lead AH109 cells to successful intravasation of tumor cells. The latter is that MUC1 of AH109A cells may be involved in the mechanism by which the cells escape from lymphocytic attack [34-36]. An example can be seen in Figure 1D, where lymphocytes seem to be unable to infiltrate in tumor cell clusters. In this aspect, we are interested in difference of Tn antigen expression in MUC1 proteins of 30~40 kDa, between primary sc tumors and metastatic tumors in the lymph nodes [Figure 8]. Since Tn antigens are immunoreactive [37-39], the difference of Tn antigen expression between primary sc tumor and lymph node-metastatic tumor supports the hypothesis that tumor cells acquire metastatic nature by changing the carbohydrates of proteins and/or lipids of cells. Our recent publication

[13] Ichikawa T, Yamamoto T, Uenishi T, Tanaka H, Takemura S, Ogawa M, Tanaka S, Suehiro S, Hirohashi K, Kubo S. Clinicopathological implications of immunohistochemically demonstrated mucin core protein expression in hepatocellular carcinoma. *J. Hepatobiliary Pancreat. Surg.*, 2006, 13: 245-251.

[14] Rahn JJ, Dabbagh L, Pasdar M, Hugh JC: The importance of MUC1 cellular localization in patients with breast carcinoma. *Cancer*, 2001, 91:1973-1982.

[15] Nassar H, Pansare V, Zhang H, Che M, Sakr W, Ali-Fehmi R, Grgnon D, Sarker F, Cheng J, Adsay V. Pathogenesis of invasive micropapillary carcinoma: role of MUC1 glycoprotein. *Modern Pathol.*, 2004, 17: 1045-1050.

[16] Kawaguchi T, Takazawa H, Imai S, Morimoto J, Watanabe T. Lack of polymorphism in MUC1 tandem repeats in cancer cells is related to breast cancer progression in Japanese women. *Breast Cancer Res. Treat*, 2005, 92: 223-230.

[17] Kawaguchi T: Cancer metastasis: characterization and identification of the behavior of metastatic tumor cells and the cell adhesion molecules, including carbohydrates. *Current Drug Targets- Cardiovascular and Haematological Disorders*, 2005, 5: 39-64.

[18] Kawaguchi T, Takazawa H, Imai S, Morimoto J, Watanabe T, Kanno M, Igarashi S: Expression of Vicia villosa agglutinin (VVA)-binding glycoprotein in primary breast cancer cells in relation to lymphatic metastasis: is atypical MUC1 bearing Tn antigen a receptor of VVA? *Breast Cancer Res. Treat.*, 2006, 98: 31-43.

[19] Tollefsen S, Kornfeld R. The B4 lectin from Vicia villosa seeds interacts with N-acetylgalactosamine residues α-linked to serine or threonine residues in cell surface glycoproteins. *J. Biol. Chem.*, 1983, 258:5172-5176.

[20] Osinaga E, Tello D, Batthyany C, Bianchet M, Tavares G, Duran R, Cervenansky C, Camoin L, Roseto A, Alzari PM. Amino acid sequence and three-dimensional structure of the Tn-specific isolectin B4 from Vicia villosa. *FEBS Lett.*, 1997, 412:190-196.

[21] Alpaugh ML, Tomlinson JS, Shao Z-M, Barsky SH: A novel human xenograft model of inflammatory breast cancer. *Cancer Res.*, 1999, 59:5079-5084.

[22] Jan YY, Yeh TS, Yeh JN, Yang HR, Chen M-F. Expression of epidermal growth factor receptor, apomucin, matrix metalloproteinases, and p53 in rat and human. Appraisal of an animal model of cholangiocarcinoma. *Ann. Surg.*, 2004, 240: 89-94.

[23] Odashima S. Establishment of ascites hepatomas in the rat, 1951-1962, In: Editor Yoshida T, Ascites Tumors-Yoshida Sarcoma and Ascites Hepatoma(s), *Natl. Cancer Inst. Monogr.*, 16, Maryland, USA, U.S. Department of Health, Education, and Welfare, 1964, 51-93.

[24] Matsushita Y., Yamamoto N, Shirahama H, Tanaka S, Yonezawa S, Yamori T, Irimura T, Sato E. Expression of sulfomucins in normal mucosae, colorectal adenocarcinomas, and metastases. *Jpn. J. Cancer Res.*, 1995, 86: 1060-1067.

[25] Hasegawa H, Kano M, Hoshi N, Watanabe K, Satoh E, Nakayama B, Suzuki T. An electrochemotherapy model for rat tongue carcinoma. *J. Oral. Pathol. Med.*, 1998, 27: 249-254.

[26] Kawaguchi T. Vicia villosa agglutinin (lectin)-binding carbohydrate(s) is expressed in atypical MUC1, serotransferrin and immunoglobulin of rat ascites hepatoma AH109A cells with lymphatic metastasis propensity. *AACR Annual Meeting Proceedings*, 2005, 46:52.

[41] Sleeman JP: The lymph node as a bridgehead in the metastatic dissemination of tumors. In: Schlag PM, Veronesi U, *Recent Results in Cancer Research* 157, Berlin, Springer-Verlag, 2000, 55-81.

Pharmaceutical Research, Vol. 25, No. 2, February 2008 (© 2007)
DOI: 10.1007/s11095-007-9398-x

Short Communication

Anti-tumor Effect of All-*Trans* Retinoic Acid Loaded Polymeric Micelles in Solid Tumor Bearing Mice

Narin Chansri,[1] Shigeru Kawakami,[1] Masayuki Yokoyama,[2] Tatsuhiro Yamamoto,[2] Pensri Charoensit,[1] and Mitsuru Hashida[1,3]

Received November 8, 2006; accepted January 18, 2007; published online July 31, 2007

Purpose. All-*trans* retinoic acid (ATRA) polymeric micelles were developed for parenteral administration. The distribution characteristics and antitumor activities of ATRA polymeric micelles were evaluated after intravenous administration to mice bearing CT26 solid tumors.
Methods. ATRA incorporated in poly(ethylene glycol)-poly(benzyl aspartate) block copolymer was prepared by the evaporation method. The levels of [^{3}H]ATRA in blood and tissue including tumor were determined by measuring the radioactivity after injection into mice. The tumor volume and the survival of the mice were determined to assess the anticancer activity.
Results. The delivery of ATRA by polymeric micelles prolonged the blood circulation and enhanced the accumulation of ATRA in the tumor tissue compared with the administration of free ATRA. Tumor growth was significantly delayed and the survival time of mice was prolonged following the treatment by ATRA polymeric micelles demonstrating the improved anticancer activity of ATRA.
Conclusion. Polymeric micelles are a promising and effective carrier of ATRA in order to enhance tumor delivery and they have a promising potential application in the treatment of solid tumors.

KEY WORDS: all-*trans* retinoic acid; antitumor activity; biodistribution; drug targeting; nanomedicine; polymeric micelles.

INTRODUCTION

All-*trans* retinoic acid (ATRA) is an active metabolite of retinoids that has been shown to exert anti-cancer activities in a number of cancer cells and tissues. The pharmacology effects of ATRA are mainly mediated by nuclear retinoid receptor that is retinoic acid receptors, leading to growth inhibition, differentiation, and apoptosis of cancer cells (1–3). Recently, it has been extensively used for the treatment of acute promyelotic leukemia (APL) (4). However, a gradual decrease in the ATRA concentration in the blood circulation after prolonged treatment and highly variable bioavailability after oral administration were observed (5,6). Therefore, parenteral formulations that maintain the ATRA concentration in the blood could enhance its pharmacological effect.

Because of the low aqueous solubility of ATRA, drug delivery carriers such as liposomes (7), emulsions (8), and solid lipid nanoparticle (9) have been employed to improve its potency and duration of activity. In particular, clinical trials have demonstrated that liposomal ATRA offers potential pharmacological advantages over the oral administration of ATRA and appears to be an effective carrier of ATRA for APL therapy (6). Recently, we have demonstrated the inhibition of pulmonary and hepatic metastasis by ATRA incorporated in cationic liposomes (10,11) and O/W emulsions (12), respectively. However, sustained circulation of the carrier for ATRA is required for maintaining the required therapeutic level and reaching the target pathological sites in the body. Therefore, the delivery of ATRA by a micelle-forming agent is represents a novel parenteral delivery system for ATRA.

Polymeric micelles are a class of micelles that are formed from block copolymers typically consisting of hydrophilic and hydrophobic polymer chains (13). They are of particular interest because of their small particle size, their efficiency in entrapping a satisfactory amount of hydrophobic drug within the inner core, their stability in the circulation and their ability to gradually release the drug (14). Furthermore, the highly hydrated outer shells of the micelles prevent reticuloendothelial system (RES) uptake and inhibit intermicellar aggregation of their hydrophobic inner cores (15). The characteristics of these polymeric micelles could be advantage for passive delivery and extravasate the drug in the tumor site by an enhanced permeability and retention effect (EPR effect) (16). In this regard, polymeric micelles have been employed to enhance *in vivo* anticancer activity by solid tumor targeting of many anticancer drugs such as doxo-

[1] Department of Drug Delivery Research, Graduate School of Pharmaceutical Sciences, Kyoto University, Sakyo-ku, Kyoto, 606-8501, Japan.
[2] Kanagawa Academy of Science and Technology, KSP East 404, Sakado 3-2-1, Takatsu-ku, Kawasaki-shi, Kanagawa 213-0012, Japan.
[3] To whom correspondence should be addressed. (e-mail: hashidam@pharm.kyoto-u.ac.jp

rubicin (17,18), camptothecin (19), paclitaxel (20), and cisplatin (21).

In our previous study, ATRA was successfully incorporated in poly(ethylene glycol)-poly(aspartate ester) (PEG-P(Asp)) block copolymer micelles in which 75% of the aspartic acid residues were esterified benzyl groups in order to increase the hydrophobicity of the inner core (22). Because ATRA is a hydrophobic drug, the interaction between ATRA and the hydrophobic inner core play a very important role in the stable incorporation. The ATRA polymeric micelles were effective in increasing the blood retention and lowering hepatic clearance compared with free ATRA and ATRA incorporated in liposomes and suggested the potential use of this system for the design of ATRA carriers in the treatment of solid tumors.

In the present study, the distribution and antitumor efficacy of ATRA incorporated in polymeric micelles was examined in mice bearing CT26 solid tumors. The distribution characteristics of ATRA delivered by polymeric micelles showed a prolonged blood retention and enhanced accumulation of ATRA at the tumor site. Finally, we evaluated the efficiency of ATRA incorporated in polymeric micelles for the treatment of solid tumors by measuring the tumor volume and survival of the mice.

MATERIALS AND METHODS

Chemical

ATRA was purchased from Wako Pure Chemicals Industry, Ltd. (Osaka, Japan). Clear-Sol I was obtained from Nacalai Tesque, Inc. (Kyoto, Japan), and Soluene 350 was purchased from Packard Co., Inc. (Groningen, The Netherlands). RPMI1640 medium was obtained from Nissui Pharmaceutical Co., Ltd. (Tokyo, Japan). Fetal bovine serum (FBS) was purchased from Biowhittaker (Walkersville, MD, USA). HCO-60 was obtained from Nikko Chemical Co. Ltd. (Japan). [^{3}H]ATRA was purchased from NEN Life Science Products, Inc. (Boston, USA). All other chemicals were of the highest purity available.

Synthesis of Block Copolymer

PEG-P(Asp) block copolymer was obtained by alkaline hydrolysis of poly(ethylene glycol)-poly(β-benzyl-L-aspatate) (PEG-PBLA) as reported previously (23). Briefly, the molecular weight of the poly(ethylene glycol) (PEG) chain was 5,000 and the average number of aspartic acid units was 27. Approximately 69% of the aspartic acid residues in the poly(aspartic acid) chain were converted to the β-amide form by alkaline hydrolysis during the synthesis of this block copolymer. A hydrophobic benzyl group was bound to 69% of the poly(aspartic acid) residues by an ester-forming reaction between benzyl bromide and PEG-P(Asp) as reported previously (24). Briefly, PEG-P(Asp) block copolymer was dissolved in *N,N*-dimethylformamide (DMF) and added to benzyl bromide along with a catalyst, 1, 8-diazabicyclo[5,4,0]7-undecene (DBU). The reaction mixture was stirred at 50°C for 15.5 h. Polymers were obtained by precipitation in an excess of diethyl ether and collected by filtration. The dried polymer was dissolved in dimethyl sulfoxide (DMSO), then 6 N HCl was added, followed by dialysis against distilled water and, finally, freeze-drying.

For determination of the polymer composition, such as the number of Asp units and the benzyl ester content, ^{1}H-NMR measurements were carried out on a 1% solution in 6D-DMSO containing 3% trifluoroacetic acid using a Varian Unity Inova NMR spectrometer at 400 MHz.

Incorporation of ATRA into Polymeric Micelles

Incorporation of ATRA into polymeric micelles was carried out by an evaporation method as previously described (22). Briefly, ATRA 1 mg and polymer 10 mg were dissolved in chloroform. After vacuum drying and desiccation, 3 ml of phosphate buffered saline (PBS) pH7.4 was added for hydration for 30 min at 25°C. The preparation was placed in the probe sonicator (200 W) for 3 min at 60°C. The obtained preparation was centrifuged at 1,500×*g* for 10 min before the supernatant was passed through a 0.450-μm filter. The maximum concentration of ATRA in the polymeric micelle preparation was about 0.066 mg/ml that quantified by the UV absorption at 340 nm after dissolving the preparation in a mixture of dimethylsulfoxide (DMSO) and water (DMSO:water=9:1 by volume). After the preparation was filtered, the concentration of ATRA in filtered preparation was adjusted to 0.060 mg/ml for *in vivo* experiments based on its UV absorption. The particle size of the polymeric micelles was measured by Zetasizer Nano Series instrument (Malvern Instruments, Ltd., Worcestershire, UK). To prepare [^{3}H]ATRA-labeled polymeric micelles, a trace amount of [^{3}H]ATRA (50 μCi) was dissolved in chloroform with ATRA and polymer and then treated exactly as described above. The filtered ATRA was adjusted to a concentration of 0.06 mg/ml based on the measured radioactivity.

Solubility of ATRA

The solubility of ATRA in serum was determined by mixing the excess amount of ATRA in serum and stirred overnight at 37°C. The undissolved ATRA was separated from the solution by filtration through 0.450-μm filter. The amount of ATRA dissolved in serum was determined by spectrophotometer at 340 nm (UV-visible Spectrophotometer, Shimazu Co., Ltd., Kyoto, Japan). The solubility of ATRA in serum was 1.426±0.009 mg/ml at 37°C (n=3).

In Vitro Cytotoxicity Experiment

3-(4,5-Dimethyl-2-thiazolyl)-2,5-diphenyl-2*H* tetrazolium bromide (MTT) assay was performed by the method described previously (10). The CT-26, mouse colon adenocarcinoma cells, was plated on a 96-well cluster dish at a density of 1×10^4 cells/0.28 cm^2. Twenty-four hours later, the medium containing various concentrations of unloaded polymeric micelles was added to the plates. After 48 h of incubation, the medium was removed and 5 mg/ml MTT solution was added to each well. Cells were incubated for 4 h at 37°C in 5% CO_2 and then 10% sodium dodecyl sulfate (SDS) solution was added followed by incubation overnight to dissolve formazan crystals. The absorbance was measured at wavelengths of 570 nm in a microplate photometer (Bio-

Rad Model 550, Bio-Rad Laboratories, Inc., Hercules, CA, USA).

In Vivo Distribution Experiment

The *in Vivo* distribution study was performed by the method described previously (25). Briefly, five-week-old male ddY mice (23–25 g) were obtained from the Shizuoka Agricultural Cooperative Association for Laboratory Animals (Shizuoka, Japan). [^{3}H]ATRA dispersed in serum or incorporated in polymeric micelles was injected into the tail vein of the mice. At each collection time point, blood was collected from the vena cava under anesthesia, and the mice were killed at the end of the experiment. Ten microliters of blood were incubated with 0.7 ml Soluene 350 overnight at 45°C. Following digestion, 0.2 ml isopropanol, 0.2 ml 30% hydrogen peroxide, 0.1 ml 5N HCl, and 5.0 ml Clear-Sol I were added in this order. The samples were stored overnight and the radioactivity was measured using a liquid scintillation counter (LSA-500, Beckman, Tokyo, Japan).

Tumor Bearing Mouse Model

Four-week-old male CDF1 mice (20–23 g) were purchased from the Shizuoka Agricultural Cooperative Association for Laboratory Animals. CT-26, mouse colon adenocarcinoma cells, were routinely grown in RPMI1640 medium supplemented with 10% FBS, 100 IU/ml penicillin, 100 μg/ml streptomycin, and 2 mM L-glutamine (all from Invitrogen Co., Carlsbad, CA, USA) in 5% CO_2 humidified air at 37°C. The cells were harvested from 2-day-old subconfluent cultures by trypsin and the cell concentration was adjusted to 10^6 cells/ml by Hank's balance salt solution (HBSS). Then, 0.1 ml of the cell suspension was inoculated subcutaneously in the lower back of each CDF1 mouse. A solid tumor was observed within 7 days after tumor inoculation.

Tissue Distribution in Tumor-Bearing Mice

The blood concentration, tissue distribution and tumor accumulation of [^{3}H]ATRA was examined in tumor-bearing mice on day 14 post-inoculation. After injection of [^{3}H]ATRA dispersed in serum or [^{3}H]ATRA polymeric micelles into the tail vein of the mice, blood, tumor and other tissues were collected and the radioactivity was determined as previously described in the *in vivo* distribution experiment.

Anti-Tumor Efficacy in Tumor-Bearing Mice

The anti-tumor efficacy of ATRA was evaluated in CDF1 mice bearing CT26 cells. We and other group demonstrated that intravenous administration of ATRA incorporated in cationic liposome, O/W emulsion, sterylglucoside liposome at dose of ATRA 0.585 or 0.600 mg/kg exhibited anti-tumor in mice model (11,12,26). Therefore, ATRA dispersed in 5% HCO-60 solution or ATRA incorporated in polymeric micelles were repeatedly injected through the tail vein at an ATRA dose of 0.600 mg/kg/day every other day from day 3 to 11 (5 doses administered) after tumor inoculation (seven mice per group). In the control group, saline (10 ml/kg/day) was administered instead of ATRA. The survival of the mice was recorded every day up to 60 days after tumor inoculation. At the same time, tumor volume and body weight were measured for individual animals as long as more than three mice survived. The tumor volume was determined by measuring the tumor diameter with calipers and calculated as follows:

$$\text{Volume} = \pi/6 \times LW^2$$

Where L is the long diameter and W is the short diameter

Statistical Analysis

Statistical comparisons were performed using Student's t test for two groups. Statistical analysis of tumor volume and survival curves was carried out using Dunnett's test and the log-rank test respectively. $P<0.05$ was considered significant.

RESULTS

Characteristics of ATRA Incorporated in Polymeric Micelles

The block copolymer was successfully synthesized from PEG-P(Asp), and about 69% of the aspartic residues were esterified with benzyl groups as reported previously (23). ATRA was incorporated into the polymeric micelles by the evaporation method, and yielded a clear solution after being passed through 0.450 μm filter. The mean particle size (volume) of the micelles after incorporation of ATRA was 36.3±0.624 (73.7±2.54%) and 290±51.9 (25.6±3.50%) (n=3), respectively. The percentage recovery of ATRA in the polymeric micelle solution detected by UV absorption at 340 nm was 14.0±2.0% (n=3) when compared with the initial amount of ATRA. As previously reported the incorporation ratio of ATRA in polymeric micelles was 96.4±0.17% suggesting ATRA almost completely incorporated in micelles (22). The particle size and concentration of ATRA in the polymeric micelle solution remained constant for at least 1 month when stored at 4°C and protected from light under nitrogen gas.

Cytotoxic Effect of Polymeric Micelles

The cytotoxicity of polymeric micelles was evaluated in CT-26 cells and no significant cytotoxicity was observed at the concentration of 2–40 μg/ml of polymeric micelles, suggesting polymeric micelles itself is low cytotoxic (data not shown).

Distribution Characteristics of [^{3}H]ATRA in Mice

Figure 1 shows the blood concentration profiles of [^{3}H]ATRA dispersed in serum (representing the inherent distribution of ATRA) and [^{3}H]ATRA incorporated in polymeric micelles after intravenous injection into mice. The blood concentration of [^{3}H]ATRA in serum was significantly lower than that of [^{3}H]ATRA in polymeric micelles over 4 h suggesting that polymeric micelles with benzyl groups can enhance the blood retention of ATRA by their encapsulation efficacy.

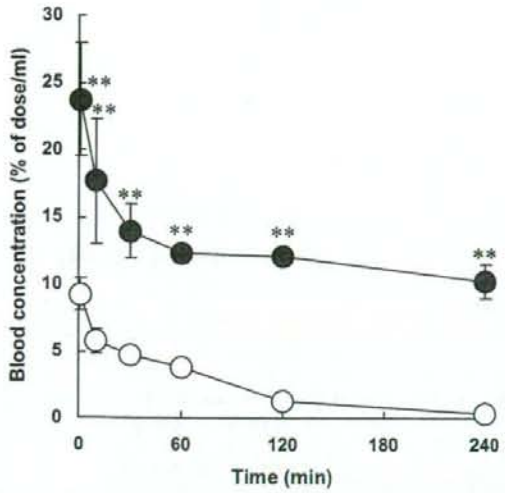

Fig. 1. Blood concentration of [^{3}H]ATRA (*open circle*) and [^{3}H]ATRA incorporated in polymeric micelles (*filled circle*) following intravenous administration to normal mice. Mice were intravenously administered with [^{3}H]ATRA dispersed in serum or [^{3}H]ATRA incorporated in polymeric micelles at 0.600 mg/kg dose of ATRA. At indicated time point, blood was collected and level of radioactivity was measured. Each value represents the mean ± SD of three experiments. Statistically significant differences compared with [^{3}H]ATRA (*double asterisk*, $P<0.01$).

Distribution of [^{3}H]ATRA in Tumor-Bearing Mice

The blood concentration and tumor accumulation of [^{3}H]ATRA dispersed in serum or [^{3}H]ATRA incorporated in polymeric micelles was evaluated in mice bearing CT26 solid tumors. The distribution of [^{3}H]ATRA was determined between 4 and 48 h after a single intravenous injection of 0.600 mg/kg ATRA. The blood concentration of ATRA in polymeric micelles was higher than that of ATRA dispersed in serum at every time point. Following a single injection of ATRA polymeric micelles, the ATRA level was prolonged to almost 48 h while ATRA dispersed in serum was rapidly eliminated and hardly any remained 24 h after administration (Fig. 2a). This sustained blood concentration of ATRA produced by polymeric micelles resulted in a higher accumulation of ATRA in the tumor tissue compared with ATRA dispersed in serum (Fig. 2b). Moreover, the liver accumulation of ATRA delivered by polymeric micelles was

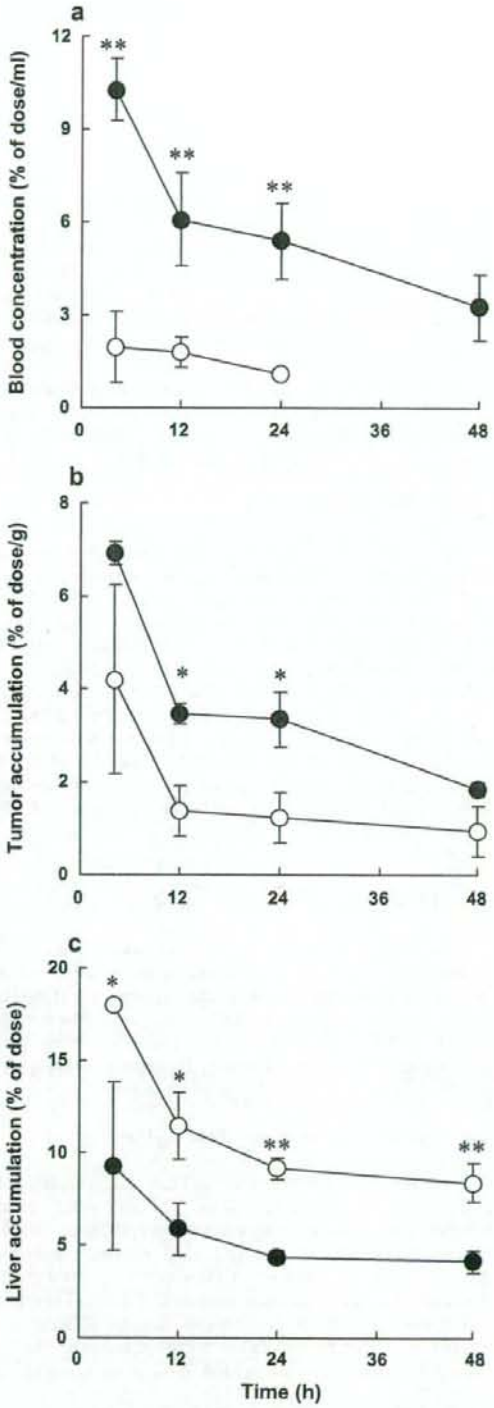

Fig. 2. Blood concentration (**a**), tumor accumulation (**b**), and liver accumulation (**c**) of [^{3}H]ATRA (*open circle*) and [^{3}H]ATRA incorporated in polymeric micelles (*filled circle*) following intravenous administration to tumor-bearing mice. Mice were intravenously administered with [^{3}H]ATRA dispersed in serum or [^{3}H]ATRA incorporated in polymeric micelles at 0.600 mg/kg dose of ATRA. At indicated time point, blood, tumor, and liver were collected and their radioactivity levels were measured. Each value represents the mean±SD of three experiments. Statistically significant differences compared with [^{3}H]ATRA (*double asterisk*, $P<0.01$; *single asterisk*, $P<0.05$).

lower than that of ATRA dispersed in serum (Fig. 2c) suggesting that polymeric micelles could reduce uptake by the liver, lead to retention in the blood and accumulate in the liver tissue. The accumulations of ATRA in lung, spleen, and kidney were very low and almost below the limit of detection within 4 h of injection (data not shown).

Anti-Tumor Effect of ATRA Incorporated in Polymeric Micelles in Tumor-Bearing Mice

The anti-tumor effect of ATRA was evaluated in mice bearing CT26 solid tumors by intravenous administration of saline (control), ATRA in HCO-60 micelles and ATRA in polymeric micelles at an ATRA dosage of 0.600 mg/kg/day or injection of 10 ml/kg/day every other day from day 3 to day 11. The body weight of mice ranged from 19 to 26 g regardless of the treatment group (data not shown). The results demonstrate that only ATRA in polymeric micelles delayed the growth of tumor lesions when compared with the controls treated with saline, while ATRA in HCO-60 micelles with the same administered dose of ATRA did not have any effect on tumor growth (Fig. 3). It was found that the tumor volume correlated with the survival of the mice and the mice died when the tumor reached around 4 cm^3. Following treatment with ATRA polymeric micelles, the survival time of tumor bearing mice was increased (median survival time=50 days) when compared with the control mice treated with saline (median survival time=29 days) and ATRA in HCO-60 micelles (median survival time=37 days; Fig. 4).

DISCUSSION

Polymeric micelles have attracted particular interest as a carrier for anti-tumor drugs, including ATRA, by enhancing drug retention in tumors by an EPR effect. Recently, Zuccari *et al.* (27) developed ATRA polymeric micelles by forming a complex of between ATRA and the modified polyvinylalcohol (PVA) substituted with oleylamine and showed enhanced

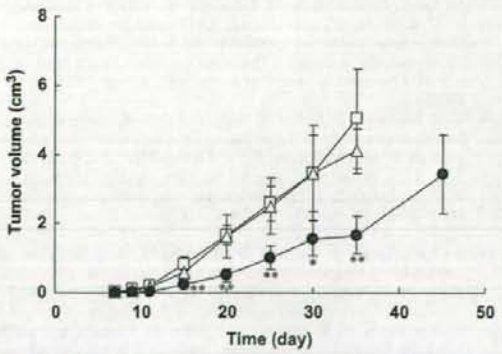

Fig. 3. The tumor volume of tumor-bearing mice after intravenous administration of saline (*open square*), ATRA in HCO-60 micelles (*open triangle*), and ATRA incorporated in polymeric micelles (*filled circle*) at 3, 5, 7, 9, and 11 days (total five doses administered) after tumor inoculation. Each value represents the mean±SD of seven mice. Statistically significant differences compared with the administration of saline (*double asterisk*, $P<0.01$; *single asterisk*, $P<0.05$).

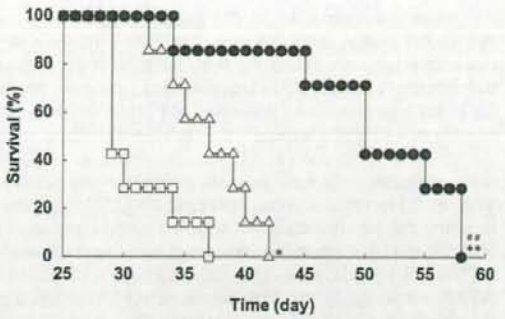

Fig. 4. Survival time of tumor-bearing mice after intravenous administration of saline (*open square*), ATRA in HCO-60 micelles (*open triangle*), and ATRA incorporated in polymeric micelles (*filled circle*) at 3, 5, 7, 9, and 11 days (total five doses administered) after tumor inoculation. Survival of mice was observed daily for 58 days and the percentage survival of each group (seven mice per group) is represented. Statistically significant differences compared with the administration of saline (*double asterisk*, $P<0.01$; *single asterisk*, $P<0.05$) and the administration of ATRA in HCO-60 micelles (*double pound sign*, $P<0.01$).

cytotoxicity of the drug towards neuroblastoma cells compared with pure ATRA. Moreover, Jeong *et al.* developed a poly(ε-caprolactone)/poly(ethylene glycol) diblock copolymer for ATRA incorporation. They examined the ATRA incorporation into polymeric micelles and ATRA release and demonstrated that the ATRA incorporation efficacy is increased by the molecular weight of hydrophobic poly(ε-caprolactone) in the poly(ε-caprolactone)/poly(ethylene glycol) diblock copolymer (28). Although these studies showed the advantages of polymeric micelles as ATRA carriers, the *in vitro* studies were not enough to provide any information about their therapeutic effectiveness. In this regard, the present study was performed to evaluate the *in vivo* efficiency of ATRA incorporated in polymeric micelles for anticancer therapy.

Since ATRA is a highly lipophilic drug (log PC_{oct}=6.6) (29), it was stably incorporated in the lipophilic inner core of the polymeric micelles and was protected from elimination by a hydrophilic outer shell. Moreover, the particle size of the prepared ATRA polymeric micelles around 160 nm provides a system to reduce elimination by the RES, prolong the retention in blood vessels, and allow passage through the leaky vasculature into the interstitial space of the tumor tissue. Therefore, the anticancer activity of ATRA would be enhanced by the incorporation in polymeric micelles.

The biodistribution of the prepared [^{3}H]ATRA polymeric micelles and [^{3}H]ATRA dispersed in serum (30,31) which represents the inherent distribution of ATRA after intravenous administration into normal mice was examined in order to compare the distribution characteristics of ATRA. As shown in Fig. 1, [^{3}H]ATRA dispersed in serum was rapidly eliminated from the blood. In contrast, [^{3}H]ATRA was significantly retained in the blood circulation when ATRA was incorporated in polymeric micelles. These results lead us to believe that when ATRA was incorporated in polymeric micelles with 69% benzyl ester groups this resulted in sustained blood concentrations of ATRA.

Since the retention in the blood circulation would benefit the passive diffusion of the molecules allowing them to accumulate in the tumor tissue by the EPR effect (16), the distribution of [^{3}H]ATRA was also evaluated in mice bearing CT26 solid tumors. The distribution of [^{3}H]ATRA in tumor-bearing mice corresponded to that in normal mice in which the blood concentration and tumor accumulation of ATRA after administration with polymeric micelles was sustained whereas the intratumor concentration of [^{3}H]ATRA dispersed in serum fell rapidly in parallel with the blood concentration (Fig. 2a and b). In addition, the lower liver accumulation of ATRA polymeric micelles (Fig. 2c) suggested a reduction of ATRA taken up by the hepatocytes or RES that benefited the retention of ATRA in the blood. Our results in prolonging the blood concentration and enhancing tumor accumulation suggested that the EPR effect plays a role in this tumor accumulation.

To investigate whether polymeric micelle-enhanced ATRA accumulated in solid tumors can improve the anticancer activity of ATRA, the therapeutic efficiency of ATRA incorporated in polymeric micelles was evaluated in tumor-bearing mice. The delayed tumor growth produced by ATRA incorporated in polymeric micelles (Fig. 3) demonstrated that ATRA incorporated in polymeric micelles exhibited superior activity against tumors compared with the administration of saline or ATRA dispersed in HCO-60 micelles. The increased survival time of tumor-bearing mice treated with ATRA in polymeric micelles compared with other treatment groups (Fig. 4) confirmed the potential therapeutic efficacy of ATRA incorporated in polymeric micelles. Altogether, these results confirmed the therapeutic efficiency of the micellar structure of PEG-P(Asp) block copolymer with 69% benzyl ester groups as an effective delivery system of ATRA to solid tumors to exert its anti-cancer activity.

One of the most interesting features of polymeric micelles is the small particle size that blocks uptake by the RES and extravasation in the tumor tissue. However, the particle size of the partial polymeric micelles in the present study was larger than previously reported (22). This may be due to the increased concentration of the prepared ATRA polymeric micelles (from 1.667 to 3.333 mg/ml) that might induce temporary aggregation of the particles during storage. However, they were small enough to escape RES scavenging and enhanced the permeability and retention at the solid tumor site since their particle size remained below 200 nm (32).

ATRA has been widely used as a chemopreventive agent, which exerts strong anti-tumor activity by suppressing tumor growth (33,34). However, like many other anticancer drugs, sophisticated delivery and targeting is required for successful *in vivo* application. Apart from the benefit with regard to the EPR effect, ATRA polymeric micelles may be able to improve the outcome of APL disease since the high plasma concentration would alleviate the progressive decline in the plasma drug concentration after prolonged oral ATRA administration. Although further study is required, ATRA incorporated in polymeric micelles could be useful for cancer differentiation therapy, including the treatment of APL in the future.

In conclusion, we have examined the biodistribution characteristics of ATRA incorporated in polymeric micelles composed of PEG-P(Asp) with 69% esterification after intravenous administration. We have demonstrated that polymeric micelles prolonged the blood retention of ATRA, produced passive accumulation in the tumor site and resulted in superior therapeutic benefits of ATRA in mice with solid CT26 tumors.

ACKNOWLEDGMENTS

This work was supported in part by Grants-in-Aid for Scientific Research and the Program for Promoting the Establishment of Strategic Research Centers, Special Coordination Funds for Promoting Science and Technology from the Ministry of Education, Culture, Sports, Science, and Technology of Japan, and by Health and Labour Sciences Research Grants for Research on Advanced Medical Technology from the Ministry of Health, Labour and Welfare of Japan.

REFERENCES

1. S. Y. Sun, and R. Lotan. Retinoids and their receptors in cancer development and chemoprevention. *Crit. Rev. Oncol. Hematol.* **41**:41–55 (2002).
2. T. Otsuki, H. Sakaguchi, T. Hatayama, P. Wu, A.Takata, and F. Hyodoh. Effects of all-trans retinoic acid (ATRA) on human myeloma cells. *Leuk. Lymphoma.* **44**:1651–1656 (2003).
3. F. Arce, O. Gatjens-Boniche, E. Vargas, B. Valverde, and C. Diaz. Apoptotic events induced by naturally occurring retinoids ATRA and 13-cis retinoic acid on human hepatoma cell lines Hep3B and HepG2. *Cancer Lett.* **229**:271–281 (2005).
4. E. Lengfelder, S. Saussele, A. Weisser, T. Buchner, and R. Hehlmann. Treatment concepts of acute promyelocytic leukemia. *Crit. Rev. Oncol. Hematol.* **56**:261–274 (2005).
5. J. Muindi, S. R. Frankel, W. H. Jr Miller, A. Jakubowski, D. A. Scheinberg, C. W. Young, E. Dmitrovsky, and R. P. Jr Warrell. Continuous treatment with all-trans retinoic acid causes a progressive reduction in plasma drug concentrations: implications for relapse and retinoid "resistance" in patients with acute promyelocytic leukemia. *Blood* **79**:299–303 (1992).
6. B. Ozpolat, G. Lopez-Berestein, P. Adamson, C. J. Fu, and A. H. Williams. Pharmacokinetics of intravenously administered liposomal all-trans-retinoic acid (ATRA) and orally administered ATRA in healthy volunteers. *J. Pharm. Pharm. Sci.* **6**:292–301 (2003).
7. E. Estey, C. Koller, A. M. Tsimberidou, S. O'Brien, M. Beran, J. Cortes, M. Tirado-Gomez, G. Lopez-Berestein, and H. Kantarjian. Potential curability of newly diagnosed acute promyelocytic leukemia without use of chemotherapy: the example of liposomal all-*trans* retinoic acid. *Blood* **105**:1366–1367 (2005).
8. S. R. Hwang, S. J. Lim, J. S. Park, and C. K. Kim. Phospholipid-based microemulsion formulation of all-*trans*-retinoic acid for parenteral administration. *Int. J. Pharm.* **276**:175–183 (2004).
9. S. J. Lim, M. K. Lee, and C. K. Kim. Altered chemical and biological activities of all-trans retinoic acid incorporated in solid lipid nanoparticle powders. *J. Control. Release* **100**:53–61 (2004).
10. S. Kawakami, S. Suzuki, F. Yamashita, and M. Hashida. Induction of apoptosis in A549 human lung cancer cells by all-trans retinoic acid incorporated in DOTAP/cholesterol liposomes. *J. Control. Release* **110**(3):514–521 (2006).
11. S. Suzuki, S. Kawakami, N. Chansri, F. Yamashita, and M. Hashida. Inhibition of pulmonary metastasis in mice by all-*trans* retinoic acid incorporated in cationic liposomes. *J. Control. Release* **116**(1):58–63 (2006).
12. N. Chansri, S. Kawakami, F. Yamashita, and M. Hashida. Inhibition of liver metastasis by all-*trans* retinoic acid incorporated into O/W emulsions in mice. *Int. J. Pharm.* **321**:42–49 (2006).
13. V. P. Torchilin. Targeted polymeric micelles for delivery of poorly soluble drugs. *Cell Mol. Life Sci.* **61**:2549–2559 (2004).